C.Yu. Zenkova, O.V. Angelsky, D.I. Ivanskyi, M.M. Chumak

Geometric phase for investigation of nanostructures in approaches of polarization-sensitive optical coherence tomography

Yuriy Fedkovych Chernivtsi National University, Chernivtsi, Ukraine, k.zenkova@chnu.edu.ua

Proposed paper presents the latest results in the framework of polarization-sensitive low-coherence interferometry related to new approaches for using the geometric phase to reproduce the polarization structure of a biological transparent anisotropic micro (nano) object. The polarization parameters of an anisotropic object are measured in real time on the basis of a modified Mach-Zehnder interferometer. The advantage of using the geometric phase is the diagnostic of polarization anisotropic surface (subsurface) nanosized layers in a non-contact, non-invasive manner

Keywords: polarization-sensitive optical coherence tomography, geometric phase, dynamic phase, thin layers of anisotropic micro (nano) objects, Mach-Zehnder interferometer.

Introduction

The 1990s were marked by new solutions of using the principles of low-coherence interferometry to obtain tomographic images of biological tissues with high spatial resolution [1, 2]. This approach, known as optical coherence tomography (OCT), has opened up additional opportunities in such areas of medical research as ophthalmology and dermatology [1, 2]. Low-coherence interferometry involves the use of broadband sources, which makes it possible to estimate the magnitude of temporal coherence and axial (longitudinal) resolution, to carry out longitudinal scanning of the biological sample under study, and to obtain topographic information about the structure of the corresponding sections [3]. The angular dimensions of the source determine the transverse resolution of the system.

The shortcomings of OCT associated with the inability to distinguish different tissues, individual nanolayers of objects, especially in a situation where such elements are damaged, destroyed or shifted, are eliminated due to an additional set of polarization measurements based on polarization-sensitive OCT (PS-OCT). The

essence of the principle of PS-OCT is a phase-polarization diagnostics of birefringent, dispersion-free, low-scattering transparent (semi-transparent) biological media, for example, the cornea of the eye [4, 5]. There are different designs of PS-OCT operating with different polarization states and different detection schemes. As a rule, PS-OCT schemes, formed on the basis of Michelson or Mach-Zehnder interferometers, implement the corresponding polarization state necessary for diagnosing of a sample, and use two detectors that record the vertical and horizontal polarization components [6].

Recent significant advances in the development of PS-OCT, combinations of this approach with other OCT approaches have made it possible to increase the sensitivity of the polarization OCT approach and improve image contrast. At the same time, there are a number of limitations in the use of PS-OCT associated with the difficulties to investigate of biological tissue surface (subsurface) nanolayers non-invasive in real time and restore information about the anisotropic nanostructure of the biological object under study.

This work presents a polarization-interference approach based on the direct measurement both of the geometric and dynamic phases in a modified Mach-Zehnder interferometer under light propagation in an

anisotropic (transparent, semitransparent) biological micro (nano) structure, which makes it possible to reproduce the geometric and polarization characteristics of nanometer-size object. It becomes possible to study thin subsurface nanolayers, 90-100 nm in thickness, multilayer biological nanostructures of various polarization and geometric properties.

I. Formation of the object beam

We consider the cornea of the human eye as an object. The main layer of the cornea [7] is its stroma, which contains about 200 parallel layers (lamellae), of 500 nm - 2.5 microns in thickness, within which collagen fibers are oriented in a certain way. According to numerous studies, lamellas can be considered as plane-parallel uniaxial birefringent micro (nano) waveplates [8, 9], characterized by a certain thickness and a certain orientation of the optical axis. The orientation of the optical axis is directly related to the orientation of collagen fibers within the lamella. We assume that the axis of the lamella is aimed at an angle of 20° with respect to the horizontal direction.

The anisotropy of the lamella refractive index Δn is determined by the geometric factor [10] $\nu = 0.32$, the difference between the refractive indices of collagen fibers ($n_{coll} = 1.47$) and the base (interstitial) substance ($n_{base} = 1.345$) is equal to 0.053. The average refractive index of the cornea according to the literature [11]: $\bar{n} = 1.375$. The thickness of the lamella layer is d≈2 μm, the surface (subsurface) nanolayers have a thickness of about 90-100 nm. The source of irradiation of the lamella S in the proposed model experiment based on the modified Mach-Zehnder interferometer (Fig. 1) is a linearly horizontally polarized beam from the source L $- \begin{pmatrix} 1 \\ 0 \end{pmatrix}$.
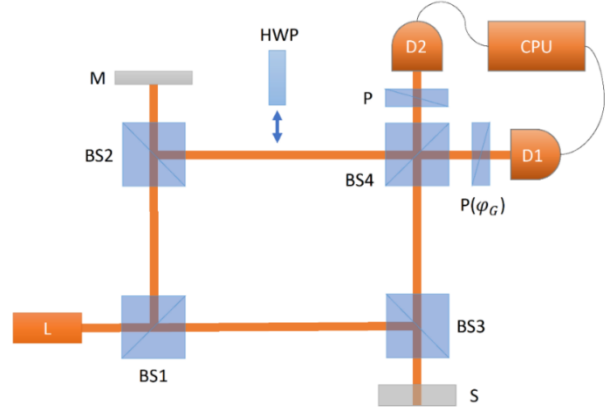

Fig. 1 Modified Mach-Zehnder interferometer for geometric phase measurement: L – light source, S – investigated sample, BS1, BS2, BS3, BS4 – beamsplitters (50/50), P(φ_G) – polarizer, which makes it possible to measure the geometric phase, D1, D2 – photodetectors in horizontal, vertical channels of the interferometer, M – mirror, HWP – half waveplate, P – polarizer, CPU – computer.

Operating wavelength ($\lambda_0 = 850$ nm) is selected for sufficient penetration of light through the retinal pigment epithelium [11]. On the other hand, the choice of the radiation source is also determined by the spectral bandwidth of the radiation source $\Delta\lambda = 170$ nm, defining the axial (longitudinal) $\delta z = l_c \frac{2\ln 2}{\pi} \frac{\lambda_0^2}{\Delta\lambda}$ and lateral (transverse) $\delta x = \sqrt{2\ln 2} \frac{2\lambda_0}{\pi} \cdot \frac{f}{\bar{n}\cdot d} = \sqrt{2\ln 2} \frac{\lambda_0}{\pi\cdot NA}$ resolution of the proposed scheme. Here $l_c = 1.36$ μm, $NA = 0.18$.

The Jones matrix of a plane-parallel uniaxial wave plate, which is a lamella model, is written as [12]:

$$M = e^{i\delta} \begin{pmatrix} \cos\frac{\gamma}{2} + i\sin\frac{\gamma}{2}\cos 2\alpha & i\sin\frac{\gamma}{2}\sin 2\alpha \\ i\sin\frac{\gamma}{2}\sin 2\alpha & \cos\frac{\gamma}{2} - i\sin\frac{\gamma}{2}\cos 2\alpha \end{pmatrix}. \qquad (1)$$

Here $\gamma = k\Delta nd -$ phase retardation, $\alpha -$ angle of optical axis orientation in a plane parallel to lamella surfaces, $\delta = k\bar{n}d$ – dynamic (mean) phase, $k = 2\pi/\lambda_0$ – wavenumber.

Interaction of polarized radiation with an object in case of reflection from its inner surface will be specified as: $\vec{E}_{ob} = M \cdot M \cdot \vec{E}_0' = \begin{pmatrix} E_{ob_x} \\ E_{ob_y} \end{pmatrix}$, where $\vec{E}_0' = \begin{pmatrix} -1 \\ 0 \end{pmatrix}$ – beam, formed due to interaction of a beam from source L with beamsplitter BS3.

The resulting Jones vector of the object beam can be represented as:

$$\vec{E}_{ob} = \begin{pmatrix} A_{ob_x} e^{i\varphi_{ob_x}} \\ A_{ob_y} e^{i\varphi_{ob_y}} \end{pmatrix},$$

where $A_{ob_{x,y}}$, $\varphi_{ob_{x,y}}$ – modulus and phase of complex amplitude components of the object field $E_{ob_{x,y}}$.

Then the parameters of the polarization ellipse of the object beam are [12]: polarization azimuth:

$$\psi = \frac{1}{2}\arctan\left(\frac{2 A_{ob_x} A_{ob_y}}{A_{ob_x}^2 - A_{ob_y}^2}\cos\Delta\varphi_{ob}\right),$$

ellipticity:

$$\chi = \frac{1}{2}\arctan\left(\frac{2 A_{ob_x} A_{ob_y}}{A_{ob_x}^2 + A_{ob_y}^2}\cos\Delta\varphi_{ob}\right),$$

where $\Delta\varphi_{ob} = \varphi_{ob_y} - \varphi_{ob_x}$.

The direction of rotation of the electric vector is determined by the sign of $\sin\Delta\varphi_{ob}$.

Major and minor axes of the polarization ellipse:

$$a^2 = A_{ob_x}{}^2 \cos^2 \psi + A_{ob_y}{}^2 \sin^2 \psi + 2A_{ob_x}A_{ob_y} \cos \Delta\varphi_{ob} \cos \psi \sin \psi,$$

$$b^2 = A_{ob_x}{}^2 \sin^2 \psi + A_{ob_y}{}^2 \cos^2 \psi - 2A_{ob_x}A_{ob_y} \cos \Delta\varphi_{ob} \cos \psi \sin \psi.$$

The result of modeling of the object beam polarization ellipse for $\alpha = 20°$, $\lambda_0 = 0.85$ μm is shown on Fig. 2.
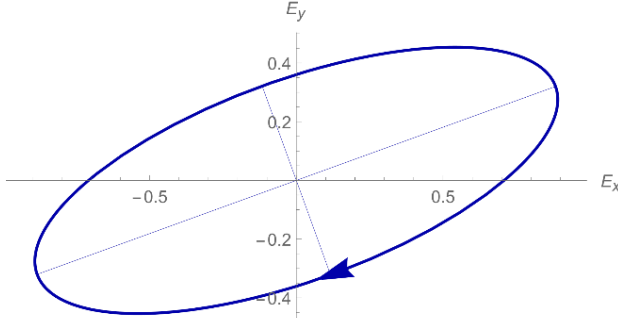

Fig. 2. Polarization ellipse of the object beam.

II. Interference approach for geometric phase retrieval

We propose a polarization-interference solution, developed within the framework of low-coherence interferometry, based on a modified Mach-Zehnder interferometer [13], which allows one to retrieve the geometric phase, which is not related to the optical path length in the medium. The geometric phase, or Pancharatnam-Berry phase, occurs when the incident polarized beam interacts with an optically anisotropic object and can be detected by an interference method. The geometric phase is determined by the parameters of optically anisotropic medium, namely the optical axis orientation and the value of birefringence. Retrieval of these parameters allows recovering information about the investigated polarization inhomogeneous anisotropic nanolayers of a biological object, which can be lost by classical schemes of the PS-OCT [14-16].

The approach proposed in this paper for restoring the geometric phase of thin nanolayers of biological objects differs significantly from the existing solutions, first of all, by the ability to study the nanometer layers of biological transparent (translucent) objects, and secondly to provide non-invasive approaches for studying of nanoobjects in real time and immediately reproduce their complex polarization structure.

In the horizontal arm of a modified Mach-Zehnder interferometer, behind the polarizer $P(\varphi_G)$ (Fig. 1) horizontal linear polarization is restored $\begin{pmatrix} 1 \\ 0 \end{pmatrix}$, repeating the polarization state at the input of the interferometer in front of the beamsplitter BS1. The horizontal arm is organized in such a way that it measures the result of interference of the reference beam with the x-component of the polarization ellipse of the object beam (Fig. 2), obtained by the interaction of an incident beam with a sample S - E_{Ob_x}. Accordingly, the vertical arm gives information about the interference of the reference beam with the y-component E_{Ob_y} of object beam (Fig. 2), which is obtained by introducing a half-wave plate HWP, in front of the polarizer P (Fig.1).

To determine the dynamic (geometric) phase and subsequent restoring of information about the object, we use the interference approach proposed in [13]. The interference distributions obtained, respectively, in the horizontal and vertical arms of the interferometer, are due to the coherent superposition of the coaxial x- and y-components. Incoherent components give an additional background of intensity, which is eliminated using additional polarizers.

In the horizontal arm of the interferometer behind the beamsplitter BS4, superposition of an object beam transformed due to reflection from this beamsplitter ($\vec{E}_{Ob}$) and incident horizontal polarization ($\vec{E}_0$), specifies the interference distribution, which is formed as a result of the superposition of coaxial components [17, 18] – E_{0_x}, E_{Ob_x}, y - component does not contribute to the interference distribution. Then the intensity distribution in the horizontal channel, taking into account the reflection coefficient r_{i_x} of incident beam with polarization $\begin{pmatrix} -1 \\ 0 \end{pmatrix}$, from the first, second surfaces (i =1, 2) of the investigated object can be written as:

$$I_{hor} = A_{0_x}^2 + \sum_{i=1}^2 A_{Ob_{x_i}}^2 + 2A_{0x}\sum_{i=1}^2 (A_{Ob_{x_i}} |\gamma(\Delta z_{opt_i})| \cos[\varphi_{hor_i}]), \tag{2}$$

where $A_{Ob_{x_i}}$ – x-component of amplitude of the reflected beam from i-th surface of birefringent object, A_{0_x} – x-component of the reference beam amplitude.

$\varphi_{hor} = \arg(E_{Ob_x} \cdot E_{0_x} e^{-i\varphi_0}) = \sum_{i=1}^2 \varphi_{hor_i}$ – the total phase in a horizontal channel. Here:
$\varphi_{hor_1} = \pi - \varphi_0$, $\varphi_{hor_2} = 2\delta + \arctan(\tan\gamma\cos 2\alpha) - \varphi_0 = \varphi_D + \varphi_G - \varphi_0$, where $\varphi_D = 2\delta$ – dynamic phase, $\varphi_G = \arctan(\tan\gamma\cos 2\alpha)$ – geometric phase (Pancharatnam–Berry phase), from which the information about birefringent medium is obtained,

$\varphi_0 = kz_0$ – reference beam phase, and $\Delta z_{opt_i} = z_{opt_i} - z_0$ – optical path difference in the interferometer arms, z_0 – optical path length of reference beam, $z_{opt_i} = 2nz_i$ - optical path length of the object beam reflected from the i-th surface. For a Gaussian spectrum, the coherence function can be written [5]: $\gamma(\Delta z_{opt_i}) = \exp(-\Delta z_{opt_i}{}^2 \Delta k^2)$, where $\Delta k = \frac{\pi}{\sqrt{\ln 2}}\frac{\Delta\lambda}{\lambda_0^2}$, where λ_0 – central wavelength, $\Delta\lambda$ – spectral bandwidth of the radiation source.

Determinative interference distribution is obtained due to reflection from the inner (second) surface of the object, so index i in the following relations will be omitted. Then from (1) it is obtained:

$$\varphi_D + \varphi_G = \varphi_0 \pm \arccos\left(\frac{I_{hor}-A_{0x}^2-A_{Obx}^2}{2A_{0x}A_{Obx}|\gamma(\Delta z_{opt})|}\right) + 2\pi m, m \in \mathbb{Z} \tag{3}$$

Information about the y-component of the object beam is considered as the result of the signal processing by the D2 detector in the vertical channel of the interferometer. Since the incident beam is horizontally polarized, when analyzing the result of interference of y-components, the reflected beam from the first surface is absent. Considering the fact that here the result of interference will be the superposition of the object beam (E_{Oby}), obtained by reflection from the second surface of the sample, and modified initial beam (E_{0y}), then the phase can be written, as:

$$\varphi_{ver} = \arg\left(E_{Oby} \cdot E_{0y} e^{i\pi} e^{-i\varphi_0}\right) = 2\delta + \frac{\pi}{2} - \varphi_0 = \varphi_D + \pi/2 - \varphi_0, \tag{4}$$

that is, it is determined as $\pi/2$ in the special experimental conditions.

Here and further we also omit the i-index. In the vertical channel, the x-component does not contribute to the result of interference. The y-component of the object beam is formed as a result of the transformation of horizontal polarization $\binom{1}{0}$ by a half waveplate (HWP), which is located in front of the beamsplitter BS4. The fast axis of the plate is oriented at an angle of 45° to the horizontal direction. The result of the superposition of coaxial y-components, taking into account reflection from the inner 2nd surface of the object will be:

$$I_{ver} = A_{0y}^2 + A_{Oby}^2 + 2A_{0y}A_{Oby}|\gamma(\Delta z_{opt})|\cos[\varphi_{ver}], \tag{5}$$

where A_{0y}, A_{Oby} - y-components of amplitude of reference and reflected beam from the 2nd surface of the object.

Thus, the dynamic phase:

$$\varphi_D = \varphi_0 \pm \arccos\left(\frac{I_{ver}-\left(A_{0y}^2+A_{Oby}^2\right)}{2A_{0y}A_{Oby}|\gamma(\Delta z_{opt})|}\right) + (2m - \frac{1}{2})\pi, m \in \mathbb{Z} \tag{6}$$

The dynamic phase (5) allows one to recalculate the geometric phase from relation (2).

We assume that $\gamma(\Delta z_{opt}) = 1$, that is, the maximum visibility of the interference distribution is achieved. Then if $\varphi_0 = \varphi_D$, the optical path difference in the arms of the interferometer is compensated.

To determine the geometric phase, we analyze the interference distributions [19], formed in the horizontal and vertical channels. We estimate the displacement of the distributions maxima relative to the starting (reference) point, that is, the position of the maximum of visibility (envelope) of the interference pattern (Fig. 3, the area is marked with a dashed line).

Figure 3 shows interferograms obtained in the horizontal (a) and vertical (b) channels of the interferometer, with a change of the reference beam phase φ_0. The footnote marks the interferogram region in the vicinity of the reference beam phase, which corresponds to the situation when an optical path difference in two arms of interferometer is compensated. This corresponds to the phase value $\varphi_0 = \varphi_D = 40.65$ rad. The shift of the interference maximum within the maximum of visibility for correlation of x-components (Fig. 3(a)) occurs, to the right (Fig. 4a, footnote), to the position of $\varphi_{hor} = 41.3$ rad. Thus, the geometric phase value:

$\varphi_G = \varphi_{hor} - \varphi_D = 0.65$ rad = 37.26°. Analogously, the analysis of the correlation of y-components (Fig. 3 (b), footnote) allows to obtain the value of $\varphi_{ver} = \frac{\pi}{2}$, which is obtained relative to the maximum of visibility determined by the dynamic phase: $\varphi_0 = \varphi_D$.

At the same time, a quadrature signal is formed in the vertical channel, the horizontal channel is connected to the geometric phase of the investigated micro (nano) object, which allows to restore the polarization properties of the object itself.

Restoring the medium parameters is as follows. From the known values of $n, \Delta n$, and the determined value of the dynamic phase, the thickness of the sample is estimated as $d = \frac{\varphi_D}{2k\bar{n}}$ and the phase retardation as $\gamma = k\Delta nd$. Here $\gamma = 0.7836$ rad $\approx 45°$. Thus, the geometric phase allows one to find the angle of the fast axis orientation of birefringent medium with respect to the horizontal direction $\alpha = \frac{1}{2}\arccos[\tan\varphi_G \cot\gamma] \approx 20°$. It should be noted that the slow axis is oriented along the collagen fibers [10], then the orientation of the fibers will be determined as $\alpha + \frac{\pi}{2}$ relative to the horizontal direction,
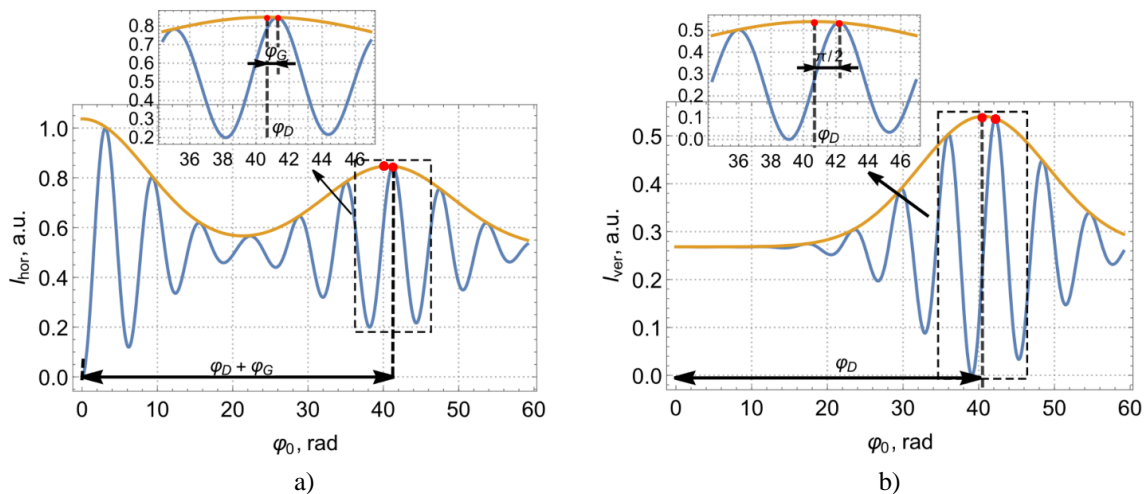
a)   b)

Fig.3. Interferograms obtained both in horizontal (a) and vertical (b) channels of the interferometer with change of the reference beam phase φ_0. The footnotes show a schematic solution for determining the geometric phase, estimated in the vicinity of the zero path difference in two arms of the interferometer.

and formed the angle above 110°.

Thus, anisotropically inhomogeneous polarization micro (nano) layers are successfully diagnosed using geometric phase approaches. This increases the accuracy of recovering information about the nanolayers geometry by 12.3%

Conclusions

Geometric phase is an additional tool for studying the polarization properties of thin polarization anisotropic layers of transparent (translucent) biological micro (nano) objects. On the basis of the modified Mach-Zehnder interferometer, an interference-polarization approach was presented, which made it possible to reproduce the polarization geometry of thin layers, in a non-contact, real time manner. This solution significantly expands the approaches of low-coherence polarization-sensitive optical tomography, in particular in increasing the reproduction accuracy of polarization information of structurally complex, polarization-anisotropic micro (nano) layers of biological objects.

Zenkova C.Y. **–** Doctor of Physical and Mathematical Sciences, professor, Department of Optics, Publishing and Printing, Yuriy Fedkovych Chernivtsi National University;

Angelsky O.V. **–** Doctor of Physical and Mathematical Sciences, professor, Corresponding member of NAS of Ukraine, Director of the Educational and Scientific Institute of Physical, Technical and Computer Sciences of Yuriy Fedkovych Chernivtsi National University;

Ivanskyi D.I. – PhD in Physical and Mathematical Sciences, Senior Researcher, Department of Correlation Optics, Yuriy Fedkovych Chernivtsi National University;

Chumak M.M. – PhD student, Department of Optics, Publishing and Printing, Yuriy Fedkovych Chernivtsi National University.

[1] A.Z. de Freitas, M.M. Amaral and M.P. Raele, *Optical Coherence Tomography: Development and Applications*. In: F. J. Duarte (ed.), Laser Pulse Phenomena and Applications (InTech, London, 2010); http://dx.doi.org/10.5772/12899.

[2] S. Aumann, S. Donner, J. Fischer, and F. Műller, *Optical Coherence Tomography (OCT): Principle and Technical Realization.* In: J. F. Bille (ed.), High Resolution Imaging in Microscopy and Ophthalmology (Springer, Cham, 2019); https://doi.org/10.1007/978-3-030-16638-0_3.

[3] M. Everett, S. Magazzeni, T. Schmoll, M. Kempe, *Optical coherence tomography: From technology to applications in ophthalmology*, Translational Biophotonics, 3(1), e202000012 (2021); https://doi.org/10.1002/tbio.202000012.

[4] M. Pircher, C. K. Hitzenberger, U. Schmidt-Erfurth, *Polarization sensitive optical coherence tomography in the human eye*, Progress in Retinal and Eye Research, 30(6), 431 (2011); https://doi.org/10.1016/j.preteyeres.2011.06.003.

[5] W. Drexler, Y. Chen, A.D. Aguirre, B. Považay, A. Unterhuber, J.G. Fujimoto, *Ultrahigh Resolution Optical Coherence Tomography*. In: Drexler, W., Fujimoto, J. (eds) Optical Coherence Tomography (Springer, Cham, 2015); https://doi.org/10.1007/978-3-319-06419-2_10.

[6] B. Baumann, *Polarization Sensitive Optical Coherence Tomography: A Review of Technology and Applications*, Appl. Sci., 7, 474 (2017); https://doi.org/10.3390/app7050474.

[7] A.J. Bron, *The architecture of the corneal stroma*, Br. J. Ophthalmol., 85, 379 (2001); http://dx.doi.org/10.1136/bjo.85.4.379.

[8] D.J. Donohue, B.J. Stoyanov, R.L. McCally, & R.A. Farrell, *Numerical modeling of the cornea's lamellar structure and birefringence properties*, Journal of the Optical Society of America A, 12(7), 1425 (1995); https://doi.org/10.1364/josaa.12.001425.

[9] M. Winkler, G. Shoa, Y. Xie, S. J. Petsche, P. M. Pinsky, T. Juhasz, D. J. Brown, & J. V. Jester, *Three-dimensional distribution of transverse collagen fibers in the anterior human corneal stroma*, Investigative ophthalmology & visual science, 54(12), 7293 (2013); https://doi.org/10.1167/iovs.13-13150.

[10] V.V. Tuchin, Tissue Optics: Light Scattering Methods and Instruments for Medical Diagnosis, (SPIE Press, Bellingham, 2015).

[11] D. A. Atchison, G. Smith, *Chromatic dispersions of the ocular media of human eyes*, Journal of the Optical Society of America A, 22(1), 29 (2005); https://doi.org/10.1364/josaa.22.000029.

[12] E. Collett, Field Guide to Polarization, (SPIE Press, Bellingham, 2005).

[13] N. Lippok, S. Coen, R. Leonhardt, P. Nielsen, and F. Vanholsbeeck, *Instantaneous quadrature components or Jones vector retrieval using the Pancharatnam–Berry phase in frequency domain low-coherence interferometry*, Optics Letters, 37(15), 3102 (2012); https://doi.org/10.1364/OL.37.003102.

[14] G. Coppola, M. A. Ferrara, *Polarization-Sensitive Digital Holographic Imaging for Characterization of Microscopic Samples: Recent Advances and Perspectives*, Appl. Sci., 10, 4520 (2020); https://doi.org/10.3390/app10134520.

[15] M.C. Pierce, M. Shishkov, B.H. Park, N.A. Nassif, B.E. Bouma, G.J. Tearney, J.F. de Boer, *Effects of sample arm motion in endoscopic polarization-sensitive optical coherence tomography*, Opt. Express, 13, 5739 (2005); https://doi.org/10.1364/OPEX.13.005739.

[16] J.N. Van der Sijde, A. Karanasos, M. Villiger, B.E. Bouma, E. Regar, *First-in-man assessment of plaque rupture by polarization-sensitive optical frequency domain imaging in vivo*, Eur. Heart J., 37, 1932 (2016); https://doi.org/10.1093/eurheartj/ehw179.

[17] O.V. Angelsky, C.Yu. Zenkova, M.P. Gorsky, N.V. Gorodyns'ka, *Feasibility of estimating the degree of coherence of waves at the near field*, Appl. Opt., 48(15), 2784 (2009); https://doi.org/10.1364/AO.48.002784.

[18] C. Yu. Zenkova, M. P.Gorsky, N. V. Gorodyns'ka, *The electromagnetic degree of coherence in the near field*, Journal of Optoelectronics and Advanced Materials, 12(1), 74 (2010).

[19] D. Lopez-Mago, A. Canales-Benavides, R. I. Hernandez-Aranda, & J. C. Gutiérrez-Vega, *Geometric phase morphology of Jones matrices*. Optics Letters, 42(14), 2667 (2017). https://doi.org/10.1364/ol.42.002667.

К.Ю. Зенкова, О.В. Ангельський, Д.І. Іванський, М.М. Чумак

Геометрична фаза для вивчення наноструктур у підходах поляризаційно чутливої оптичної когерентної томографії

Чернівецький національний університет імені Юрія Федьковича, м. Чернівці, Україна, k.zenkova@chnu.edu.ua,

Представлена робота пропонує останні результати в рамках поляризаційно чутливої низькокогерентної інтерферометрії, пов'язані з новими підходами по використанню геометричної фази для відтворення поляризаційної структури біологічного прозорого анізотропного мікро- (нано-) об'єкта. Було показано, як на базі модифікованого інтерферометра Маха-Цандера, вимірюються поляризаційні параметри анізотропного об'єкта у реальному масштабі часу. Перевагою використання геометричної фази є можливість діагностики поляризаційно-анізотропних поверхневих (підповерхневих) шарів нанорозмірів безконтактним, неінвазивним чином.

Ключові слова: поляризаційно чутлива оптична когерентна томографія, геометрична фаза, динамічна фаза, тонкі шари анізотропних мікро- (нано-) об'єктів, інтерферометр Маха-Цандера.